2017

Simulation of Human Ankle Trajectory during Stance Phase of Gait

Leslie Castelino
Michigan Technological University, lcasteli@mtu.edu

SIMULATION OF HUMAN ANKLE TRAJECTORY DURING STANCE PHASE OF GAIT

By

Leslie Castelino

A REPORT

Submitted in partial fulfillment of the requirements for the degree of

MASTER OF SCIENCE

In Mechanical Engineering

MICHIGAN TECHNOLOGICAL UNIVERSITY

2017

This report has been approved in partial fulfillment of the requirements for the Degree of MASTER OF SCIENCE in Mechanical Engineering.

Department of Mechanical Engineering – Engineering Mechanics

Report Advisor: *Mo Rastgaar*

Committee Member: *Ossama Abdelkhalik*

Committee Member: *Steven J. Elmer*

Department Chair: *William W. Predebon*

Table of Contents

Acknowledgement

I express my sincere gratitude to my advisor, Dr. Mo Rastgaar for this opportunity. His undulating support and guidance has been paramount throughout my research project.

I thank the members of the Human Interactive Robotics Laboratory, including Guilherme Ribeiro, Lauren Knop, Dr. Evandro Ficanha and Dr. Houman Dallali for their best efforts in building and developing the simulation. Thank you for guiding me and providing timely solutions to my problems.

Lastly, I thank my family and friends for their support.

Abstract

A simulation was developed which mimics the human gait characteristics based on the input of an individual's gait trajectory. This simulation also estimates the impedance of the human ankle based on the ground reaction forces measured by the force plate. This simulation will accept alterations of the following parameters: total body weight, weight of the shank, weight of the foot, trajectories of the shank and foot of the individual and orientation of the force plate, which would generate a new gait trajectory for the ankle during the stance phase of gait. The goal of this simulation was to validate the protocols followed during experiments conducted on human participants to estimate the impedance of the ankle. It also allowed us to understand and explore different system identification methods. The gait data of two individuals measured experimentally was used to build this simulation model. The simulation implements proportional-integral-derivative (PID) control and impedance control to regenerate the ankle trajectories with time-varying impedance of the ankle joint. This model was tested using the trajectories of the shank and foot from two additional individuals and replicated experimentally obtained ankle trajectories of these individuals, with a mean relative error of 0.53±0.3%, 5.74±4.85% and 4.94±3.13%, in ankle translational trajectory and ankle angular trajectories in dorsi-plantarflexion and inversion-eversion respectively.

1. Introduction

Approximately two million people live with limb amputations in the United States, of which below knee amputations are the most common [3]. Unilateral below-knee amputees, who use passive prosthesis, rely more on their hip joint for walking thereby exerting 20 to 30 percent more metabolic energy than non-disabled people do, for the same speed of gait. This leads to a 30 to 40 percent reduction in their preferred speed of gait in comparison to non-disabled people [4-5]. Herr and Grabowski [6], and Ferris and Aldridge [7] show that providing adequate power during push-off, using a powered ankle-foot prosthesis, reduces the additional metabolic energy required by unilateral transtibial amputees for straight walking. Ordinary gait activities also include other gait patterns such as turning, walking on slopes and uneven terrain, which are complex in nature. Since single degree of freedom ankle actions are uncommon in normal gait activities, control of multiple ankle degrees of freedom offers exceptional challenges [13]. Although turning steps account for 8 to 50 percent of all steps performed during daily activities [33], most research is focused on straight walking. Modulation of ankle impedance in the sagittal and frontal planes is pivotal during turning, as it helps in regulating the ground reaction forces which are larger during a turning step than during a straight step [8]. This inconsistency in ground reaction forces results in different gait patterns between people with amputations who use a passive prosthesis to increase mobility and non-disabled people [14]. Hence, in improving the design of ankle-foot prostheses, understanding the ankle impedance in more than one direction of movement during gait is vital.

Mechanical impedance of a system is the relationship between the input motion and the correlated resultant torque. It is a function of the systemic parameters i.e. stiffness, damping and inertia. Ankle mechanical impedance is a time-varying function that relates the ankle's angular motion with the correlated resultant torque at the ankle joint. Controlling the ankle impedance in dorsi-plantarflexion (DP), inversion-eversion (IE), and external-internal (EI) degrees of freedom facilitates an unimpaired human to achieve locomotion. This indicates that an ankle-foot prosthesis with multiple degrees

of freedom and dynamic impedance, leads to an agile gait similar to the unimpaired human ankle. Using better design features and control methods, a more efficient gait may be achieved that allow walking on slopes and uneven terrain by conforming the foot to the ground profile.

New ankle-foot prostheses are conceived by understanding the ankle's capability of modulating impedance in multiple degrees of freedom during the stance phase of gait [9-12]. Currently, powered ankle prosthesis controllers are built on ankle torque-angle relations that are averaged across a study population [16] rather than ankle impedance. Under non-load bearing and stationary conditions, mechanical ankle impedance by Rastgaar et al. [17-18] and quasi-static mechanical impedance by Lee et al. [18] in both DP and IE directions were estimated. Rouse et al. [23-24] estimated ankle impedance during the stance phase in the sagittal plane by applying perturbations using a Perturberator robot.

Ficanha and Rastgaar [15, 25] developed an impedance controlled cable-driven ankle-foot prosthesis controllable in DP and IE directions. Lee et al. [19-22] and Ficanha et al. [26] developed a method for estimating the time-varying ankle mechanical impedance in the sagittal and frontal planes for straight walking. The work discussed here is a simulation of straight walking gait pattern of human participants who participated in the above mentioned experiment. This involved animating the experimentally recorded human ankle motion [1] using a model of the cable-driven ankle-foot prosthesis [15]. The simulation mimicked the ankle trajectory of the participants and helped validate the protocols followed during the experiments in the laboratory. It also simulated different gait scenarios by varying the impedance of the ankle, which facilitated the understanding of the effects of impedance on the human gait pattern. This simulation envisions to create a platform for testing the ankle-foot prosthesis thereby eliminating the need for conducting experimental trials with lower-extremity amputees.

2. Experimental Procedure

Experiments on human participants [26] were conducted using an instrumented walkway [2] to track the human ankle kinematics and kinetics for straight walking. A motion-capture system consisting of eight Opti-Track Prime 17W cameras (NaturalPoint Inc; Corvallis, Oregon) was used to track the gait patterns of the participants. The cameras were oriented in a square formation covering a volume of about 16 m^3 and an area of 12 m^3. The cameras emitted infrared light and captured the light reflected off the reflective markers that were mounted on polycarbonate plastic rigid frames at 350 Hz, which is the maximum sampling frequency of the motion-capture system. One polycarbonate plastic rigid frame was placed on the shoe of the participant and another was placed on the shinbone of the shank to record the global position and orientation of the foot and shank respectively. The ankle position and orientation were estimated as the relative motion of the foot with respect to the shank.

To measure the kinetics of the human ankle, the participants walked on a perturbation platform which consisted of a Type 5233A force plate (Kistler® 9260AA3) mounted on a universal joint and supported by four high stiffness springs with stiffness of 12000 N/m, one at each corner as shown in *Figure 1(b)*. The position of the force plate is measured using infrared markers *(Figure 1(a))* attached to the top of the force plate. The force plate module had four individual load cells located at each corner which would sense the force exerted by the foot and identify the center of pressure of the foot. The force plate was actuated through Bowden cables which were connected to two linear voice coil actuators (Moticont® GVCM-095-089-01). The voice coils rotate to push or pull the Bowden cables which cause the force plate to rotate with two degrees of freedom (lateral and sagittal plane). The participants performed the experiment at their self-selected speed of gait and their speed was kept consistent using a metronome. The participant would then walk on the platform with the force plate being actuated just before heel-strike. The perturbation platform was set up in such a way that just before contact with the foot, the force plate module was actuated resulting in a stochastic torque being applied to the foot in DP and IE directions. The ground reaction

forces of the foot were measured from the force plate in the force plate coordinate system. The origin of the force plate coordinate system coincided with the origin of global coordinate system of the motion capture system. The data from the force plate was obtained at 3500 Hz using LabVIEW® [29] and National Instruments data acquisition system and down sampled to 350 Hz to synchronize the force plate data with the motion-capture data. This also eliminates the high frequency noise components from the force plate data. The experiments provided data of the position and orientation of the shank and the foot which were used to compute the resulting position and orientation of the ankle. The forces and torques measured from the force plate helped estimate the forces and torques acting on the ankle.

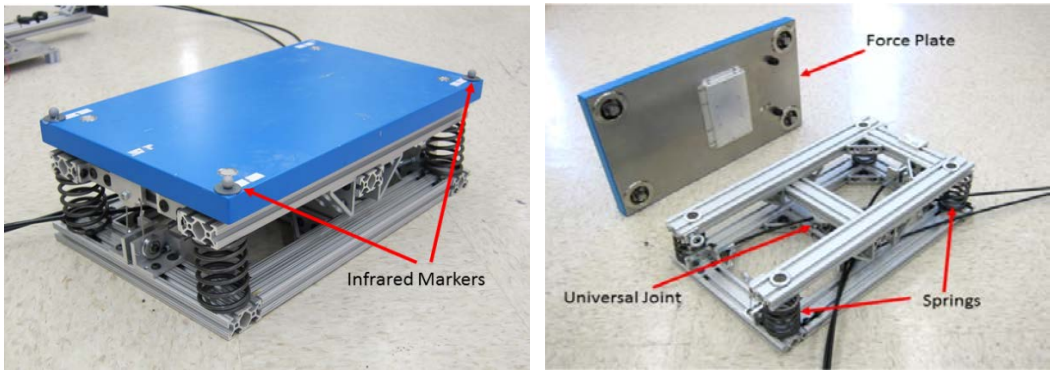

Figure 1(a). Force Plate Module

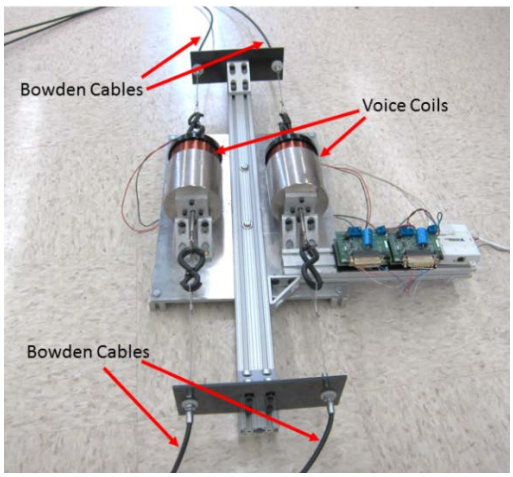

Figure 1(b). Actuation Module

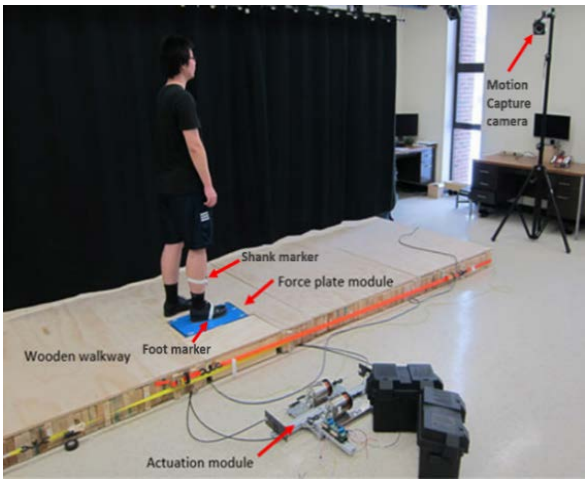

Figure 1(c). Experimental Setup
MTU Human-Interactive Robotics Lab

3. Simulation Model

The simulation model, consisting of two-degree of freedom ankle-foot prosthesis and instrumented perturbation platform, was modeled in SOLIDWORKS® [31] with 8 degrees of freedom as shown in *Figure 2*. The mass and inertia properties of the shank and the foot are shown in *Table 1*. The hip had one rotational degree of freedom in the transverse plane, whereas the knee and ankle had two rotational degrees of freedom each, in the lateral and sagittal planes. The ankle-foot prosthesis was mounted on a guideway system that had three translational degrees of freedom in the Cartesian coordinate system. The SolidWorks model was exported to Simulink using the Simscape Multibody Link, which generated a second generation SimMechanics model in Simulink with prismatic joints representing the translational degrees of freedom and revolute joints representing the rotational degrees of freedom. The Cartesian coordinate frame with X representing the forward motion, Y representing the ascending and descending motion and Z representing the lateral motion was used as the reference coordinate system. The ankle rotations in plantarflexion, eversion and supination of the right foot were considered to be positive perturbations.

The model was actuated by data obtained from experiments conducted on human participants using the instrumented perturbation platform using the force plate module and motion capture system. The position and orientation of the ankle joint was derived from experimental data which included position and orientation of the shank and foot. Considering the ankle as the end effector of the system and implementing inverse kinematics, the position for each of the six joints of the model was calculated from the position and orientation of the ankle. Hence, the time history of the ankle joint trajectory provided the time history for the knee and hip trajectories. The weight of the shank and foot, along with the weights representing total body weight of the person, were variable, which helped achieve a gait pattern that more accurately resembled the participant's gait pattern. Three methods of input to the ankle joint were used to mimic the ankle trajectory. In the first control method, the ankle joint was actuated in DP and IE directions, using the position data derived from the trajectory of the shank and foot.

In the second method, the ankle joint was actuated using PID control with position feedback. In the third method, using impedance control, the ankle joint was actuated using a torque calculated based on the desired impedance of the ankle joint. Each simulation imitated three steps on the walkway, which included one step on the force plate and one step each before and after the force plate.

Since the system required a stiff solver, the ode23tb solver which implements the Trapezoidal Backward Differentiation Formula (TR-BDF2) method was found to be the best suited solver among the built-in Simulink solvers. The solver was set to variable-step type with a maximum step size of 0.001. Since the revolute and prismatic joints represented physical systems, the input to these joints had to be physical system signals. A Simulink to Physical System Converter block was used to convert the Simulink signal to a Physical System signal. Similarly, a Physical System to Simulink Converter block was used to convert the physical signals back to Simulink signals. In the force plate module, the spring joints with stiffness of 12000 N/m and the universal joint with stiffness of 270 N-m/deg in DP and 150 N-m/deg in IE [2] were modeled. Damping on these joints was set to 1 N-m-s/rad. The stiffness and damping on the prismatic and revolute joints representing the guideway system and the hip and knee respectively was set to zero. The revolute joints representing ankle rotations in DP and IE had variable stiffness and damping parameters to modulate the impedance of the ankle during the simulation.

$$T_{FP} = J_F\ddot{\theta}_F + B\dot{\theta}_A + K\theta_A \qquad (1)$$

The torque acting on the ankle is explained by *Equation (1)*; where $\theta_A, \dot{\theta}_A$ are the angular displacement and velocity of the ankle respectively. B and K are the stiffness and damping of the ankle joint. T_{FP} is the reactive torque experienced by the force plate which consists of both the torque generated by the perturbations as well as the individual's effort which is uncorrelated to the ankle kinematics. J_F and $\ddot{\theta}_F$ are the inertia and angular acceleration of the foot which are not estimated in this study.

Element	Shank	Foot
Mass (kg)	2.5±0.001	1±0.001
I_{xx} (kg-m^2)	2.087e-2	2.623e-4
I_{yy} (kg-m^2)	2.814e-4	1.091e-3
I_{zz} (kg-m^2)	2.087e-2	8.351e-4
I_{xy} (kg-m^2)	0	-3.987e-6
I_{yz} (kg-m^2)	0	-1.388e-7
I_{zx} (kg-m^2)	0	-2.566e-5

Table 1. Mass and Inertia properties of the shank and foot

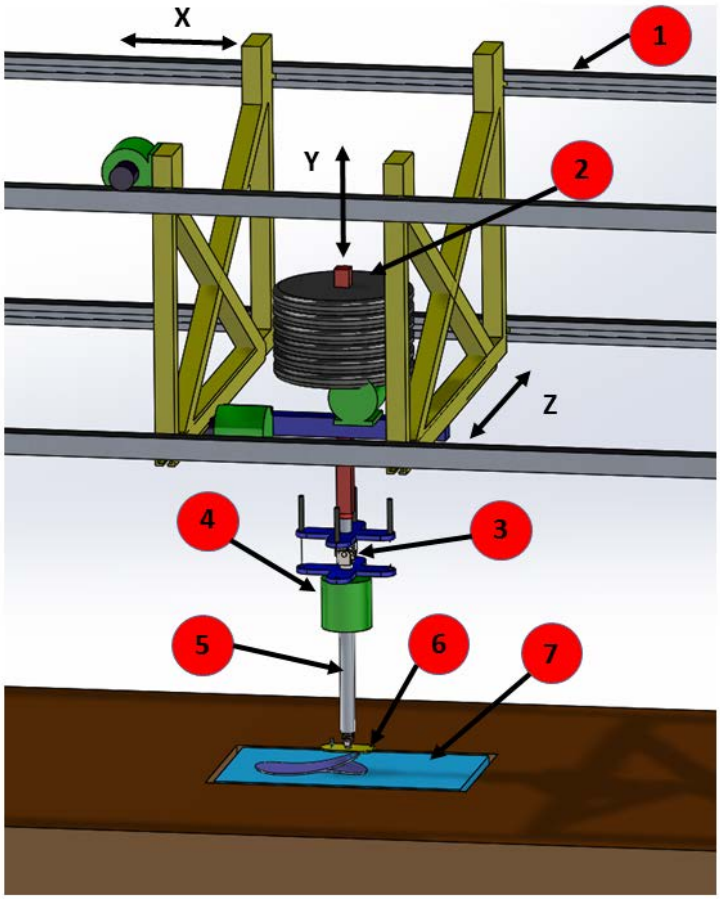

Figure 2. Simulation model: (1) Guideway (2) Weights (3) Knee (4) Hip motor (5) Shank (6) Foot (7) Force Plate

3.1. Ground Contact Model

The interaction of the foot with the ground surface was modeled as a stick-slip friction model. The contour of the base of the prosthetic foot was approximated to have 13 points of contact *(Figure 3)*. Based on the position and orientation trajectory of the ankle and the corresponding forces and torques acting on it, the ground contact dynamics were estimated. The normal reactive force acting on every point was calculated according to *Equation (2)*, where F_N represents the normal reactive force, K and B represent stiffness and damping, and y and v represent the virtual position and velocity of the point with respect to the ground surface.

$$F_N = -K * y - B * v \qquad (2)$$

To imitate the corporeal interaction of the foot with the ground surface, each point of contact was designed as a spring-damper model with stiffness and damping of 200,000 N/m and 2,000 N-s/m respectively. This was in agreement with previously reported results [32]. Stiffness was quantified only for normal reactive force whereas damping was quantified for normal as well as shear reactive forces. At the point of contact, depending upon the virtual distance of these points on the foot from the ground surface, the extent of compressive force the foot applied on the surface was calculated. These forces were translated to the ankle joint and corresponding torques were calculated. The reactive force generated at each contact point attempted to simulate the interaction of the foot with the ground surface during the experiments.

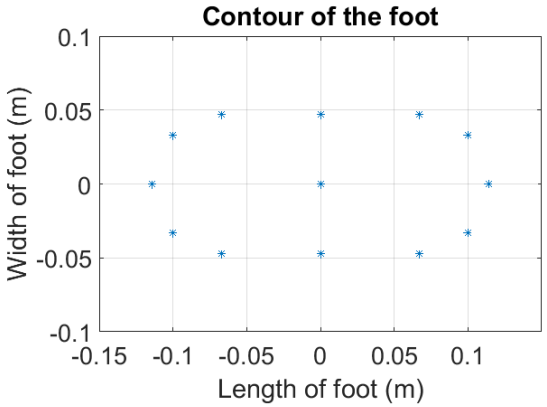

Figure 3. Contour of the base of the prosthetic foot

4. Control Methods

4.1. Feedforward Position Input Method

The six degrees of freedom of the model were actuated using position as the feedforward input. All revolute joints and prismatic joints representing the rotations of the hip and the knee and the translation of the guideway system respectively, were actuated by position input. From the position of the ankle, the position of each joint was calculated using inverse kinematics. A delay of one sample had to be introduced to lower the computation time and avoid algebraic loops. Position input method was a brute force method which caused every joint to follow the gait trajectory ignoring the reactive forces acting on the joints as a result of the interaction with the environment. During the stance phase, the ground contact model consumed enormous computing time to calculate the ground reaction forces. Since the ankle joint was not controlled using torque feedback, very large ground reaction forces were experienced on the foot. The angular joints at the ankle in the frontal and sagittal plane were also actuated by position. The block diagram of feedforward position input method is shown in *Figure 4*. Although this method did not simulate the corporeal interaction of the foot with the ground surface, it aided the process of understanding and revising the working principle of the ground contact model. This method also assisted in improving the inverse kinematics calculations.

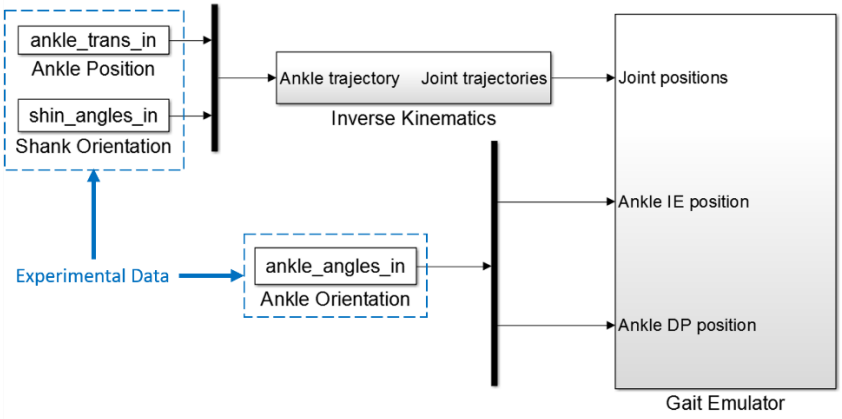

Figure 4. Block Diagram of Feedforward position input method

4.2. Position Control using Proportional-Integral-Derivative (PID)

To overcome the disadvantages of feedforward position input, the prismatic joint controlling the vertical position of the prosthesis in the Y axis, was actuated using force input. The revolute joints representing the hip and knee, and the prismatic joints representing the translation of the guideway system in the X and Z axes, were actuated by position input computed using inverse kinematics. The position input for the Y axis prismatic joint, computed using inverse kinematics, was used as an input to a PID block. The PID block used the error between this desired position and the current position feedback of the prismatic joint, to calculate the force input to the prismatic joint. To achieve the swing phase of gait, the output of the PID block was used as the force input to the Y axis prismatic joint. During the stance phase of gait, the force input to the prismatic joint was set to zero. This ensured that the entire weight of the prosthesis was acting on the ground surface and that no force was acting against gravity. To switch the input to the prismatic joint during the swing and stance phases, a switch block was used. There were three inputs and one output in the switch block. The first and third inputs were the two choices of force inputs to the prismatic joint, one from the PID block output and the other set to zero. The switching mechanism was controlled by the second input which was the ground reaction force which detected the start and end of the stance phase. The ground reaction force was computed using the ground contact model. Throughout the stance phase, starting from heel strike and ending with push-off, the ground reaction force was greater than zero. During the swing phase, as there was no contact between the foot and the ground surface, the ground reaction force was zero. The force control module on the Y axis prismatic joint is shown in *Figure 5*.

The two revolute joints controlling the rotation of the ankle in DP and IE were controlled using one PID block for each joint. The PID block provided the input torque for the ankle joints by computing the error between the desired ankle angular rotation and the current ankle angular rotation. The PID block provides admittance at the ankle joint, thus producing a better interaction of the foot with the ground surface. The block diagram of the PID controller is shown in *Figure 6*. The impedance of the ankle varies

with time. Impedance at five instances of the stance phase was experimentally estimated [26]. This time-varying impedance at specific intervals of the stance phase was transformed into a curve which shows how impedance changes across the stance. This curve was used to change the impedance of the ankle in real-time and simulate the ankle trajectory.

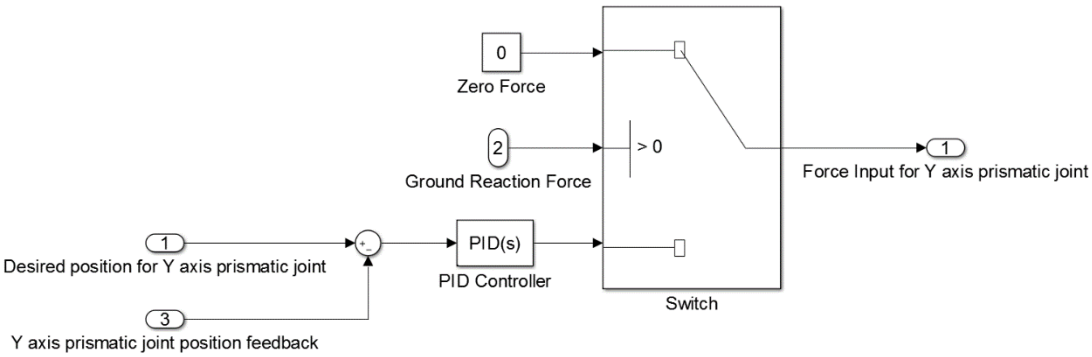

Figure 5. Control Loop for Force Control on Y axis prismatic joint

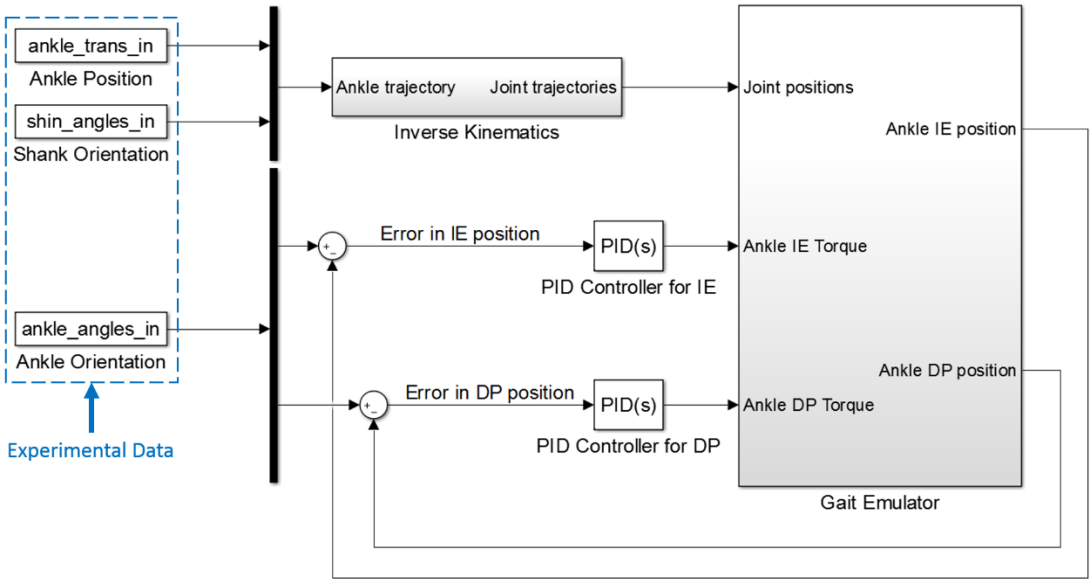

Figure 6. Block Diagram of Position Control on Ankle Joint using PID

4.3. Impedance Control

The objective of an impedance controller [27] is to enforce a desired dynamic relation, impedance of the interaction, between the manipulator end-effector and its environment. A second order impedance model, expressed by *Equation (3)*, was chosen.

$$M_d\left(\ddot{\theta} - \ddot{\theta}_d\right) + B_d\left(\dot{\theta} - \dot{\theta}_d\right) + K_d(\theta - \theta_d) = -F_e \qquad (3)$$

M_d, B_d and K_d are constant diagonal and positive definite matrices representing the desired inertia, damping and stiffness system matrices. $\ddot{\theta}_d$, $\dot{\theta}_d$, θ_d and $\ddot{\theta}$, $\dot{\theta}$, θ are the desired and current end-effector positions, velocities and accelerations respectively. F_e is the generalized external force exerted by the environment on the end-effector. When the end-effector follows an acceleration $\ddot{\theta}_r$ computed by *Equation (4)*, the manipulator behaves according to *Equation (3)*.

$$\ddot{\theta}_r = \ddot{\theta}_d + M_d^{-1}\left[-F_e + B_d\left(\dot{\theta}_d - \dot{\theta}\right) + K_d(\theta_d - \theta)\right] \qquad (4)$$

The ankle joint is then actuated using torque input calculated in joint space using inverse dynamics as expressed in *Equation (5)*.

$$u = J^T(q)\, F_e - [M(q)\ddot{q} + C(q, \dot{q}) + g(q)] \qquad (5)$$

$M(q)$, $C(q, \dot{q})$ and $g(q)$ are the mass matrix, Coriolis force matrix and gravitational force matrix of the system in joint space which were computed in symbolic form using Robotran software [28]. $J(q)$ is the Jacobian of the foot with respect to the ankle joint and $\ddot{q}$ are the angular accelerations of the ankle joint in DP and IE. u is the torque input applied at the ankle joint in DP and IE.

The revolute joints representing the hip and the knee, and the prismatic joints representing the translation of the guideway system in the X and Z axes, were actuated by feedforward position input computed using inverse kinematics. In Robotran, a model of the foot with mass and inertia properties obtained from SOLIDWORKS was used to obtain the mass matrix, Coriolis force matrix and gravitational force matrix of the system in joint space. The manipulator was realized with the foot as the end-effector

and ankle rotations in DP and IE as the manipulator joints. The position and orientation trajectory of the foot was obtained from the motion capture data. The ankle kinematics which include current angular position, velocity and acceleration of the ankle joint, and ground reaction forces and torques which are external forces and torques acting on the foot were used to compute the mass matrix, Coriolis force matrix and gravitational force matrix at a particular instant. The current simulation time was used to determine the current stage of the stance phase. Experimentally estimated impedance of the ankle at five instances of the stance phase [26] was used as the time-varying impedance of the ankle joint. According to *Equation (4)*, using the desired and current foot kinematics which are the angular position and velocity of the foot, for a desired impedance of the ankle joint, the desired angular acceleration of the foot was computed. For a desired impedance of the ankle joint, the impedance control algorithm computed the torque required at the two revolute joints controlling the rotation of the ankle in DP and IE. *Figure 7* shows a block diagram of the impedance controller design.

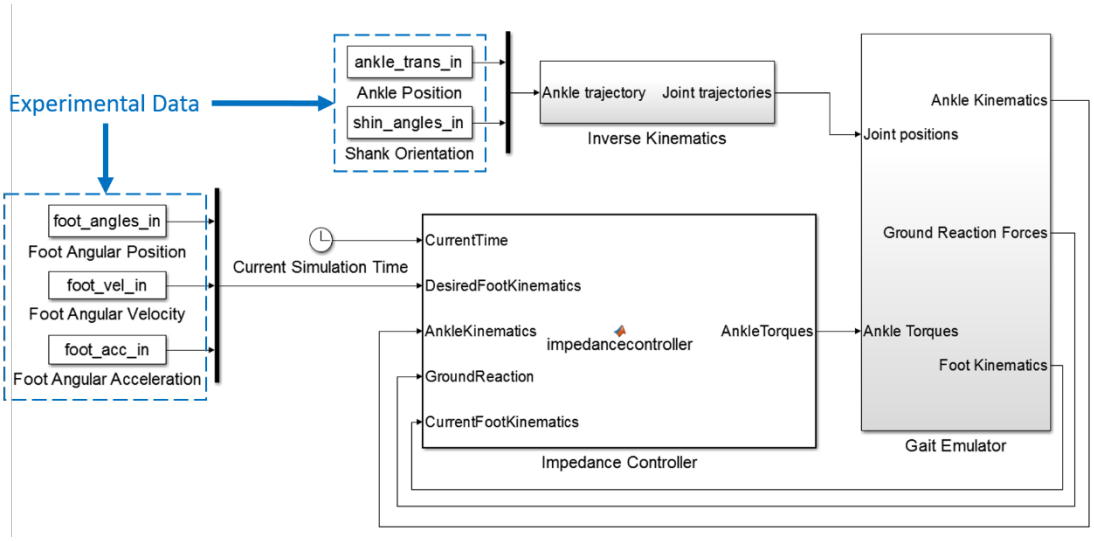

Figure 7. Block Diagram of Impedance Control on Ankle joint

5. Results

5.1. Impedance estimation during standing

In the simulation, the prosthesis was placed directly above the center of the force plate and the force plate was actuated using stochastic torque input in the DP and IE directions simultaneously. The stiffness and damping parameters of the revolute joints representing the hip and knee were set to zero. The stiffness on the X, Y and Z prismatic joints was set to 10,000 N-m/deg, 100 N-m/deg and 100 N-m/deg respectively. The damping on all prismatic joints was set to 1 N-m-s/deg. The ankle joint was passive and its stiffness in DP and IE directions was set to a range of desired values which remain constant throughout one simulation cycle. The simulation runs for 10 seconds and estimates the stiffness and damping of the ankle joint in DP and IE by measuring the ground reaction forces exerted by the force plate on the foot.

Experimentally [2], the quasi-static impedance was estimated to be 319 N-m/rad and 119 N-m/rad in DP and IE respectively. In the simulation model, the stiffness of the ankle joint was varied from 250 N-m/rad to 350 N-m/rad and 50 N-m/rad to 150 N-m/rad, in DP and IE respectively, in 20 equally spaced intervals. Ground reaction forces and torques from the force plate and the angular displacement of the ankle joint in DP and IE were measured. The ground reaction forces were transformed to torques acting on the ankle. The relationship between angular displacement of the ankle and reactive torque acting on it was approximated to be linear and a linear fit regression model was used to evaluate the stiffness. *Figure 8* shows the estimated stiffness to be fairly similar to the actual stiffness of the ankle. The R^2 values for the linear fit were always above 96% as shown in *Figure 9*. The percentage error in estimation of stiffness was found to be less than 0.47% in DP and 1.6% in IE. This shows that the relationship between reactive torque and angular displacement of the ankle is fairly linear and hence validates the experimental model used to estimate the stiffness of the ankle. *Figure 10* shows the difference between the estimated torque at the ankle and the simulated torque acting on the ankle. The difference was due to small numerical errors in computing the

high frequency transient torque acting on the ankle. *Figure 11* shows the difference between the simulated torque acting on the ankle (measured from the ankle joint in the simulation) and the estimated torque (measured from the force plate in the simulation) for a desired ankle stiffness of 319 N-m/rad and 119 N-m/rad in DP and IE respectively.

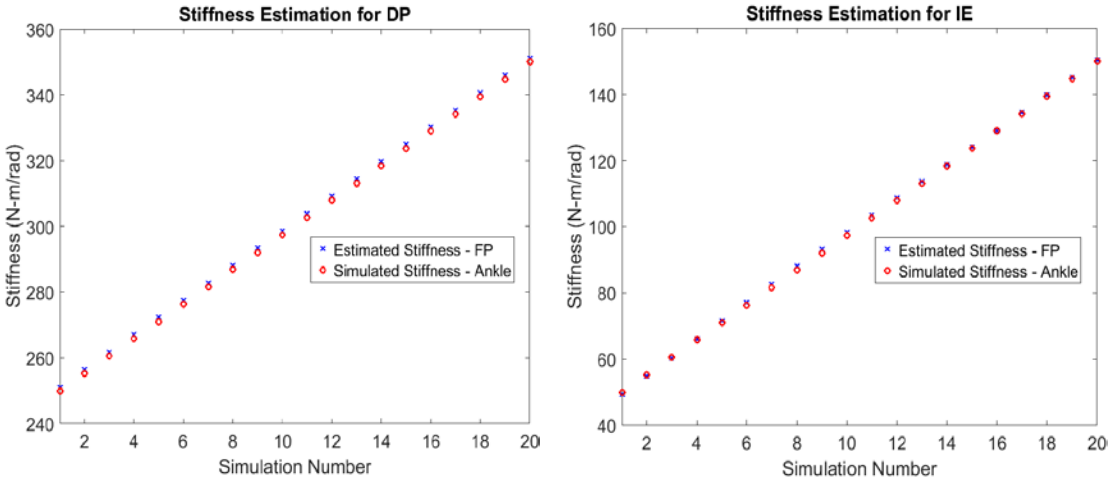

Figure 8. Estimation of ankle stiffness in DP and IE

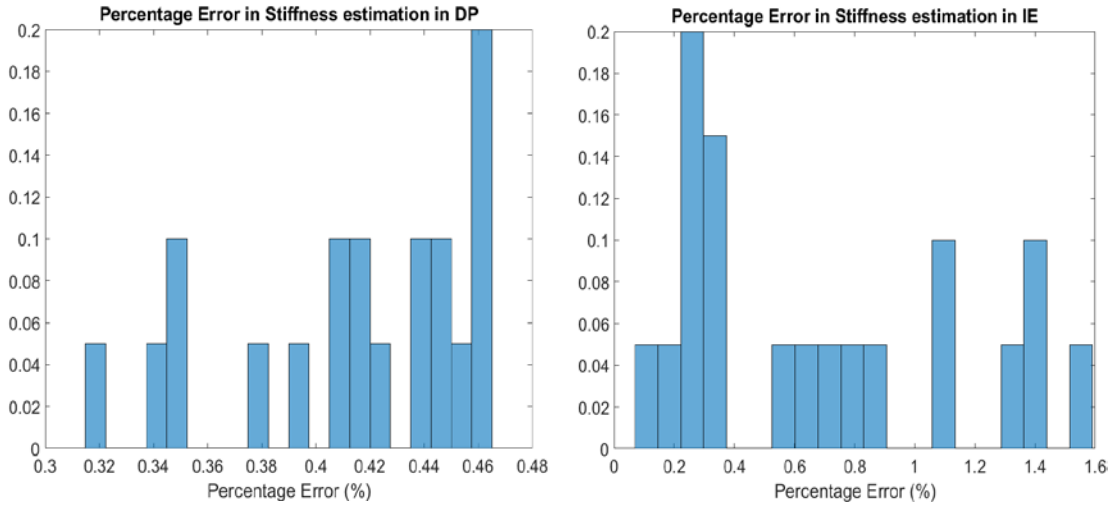

Figure 9. Relative Error histogram for estimation of ankle stiffness in DP and IE

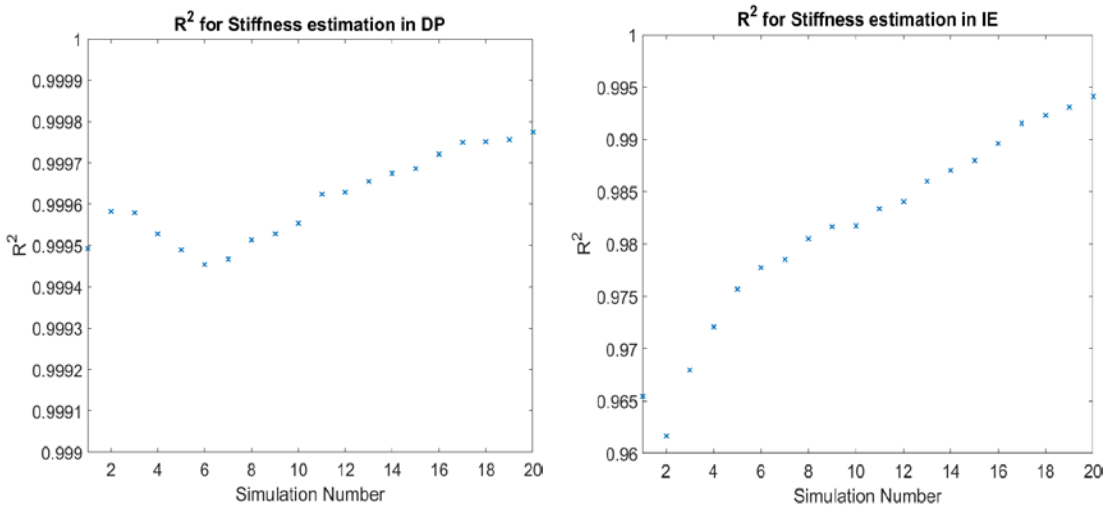

Figure 10. Regression values in estimation of ankle stiffness in DP and IE

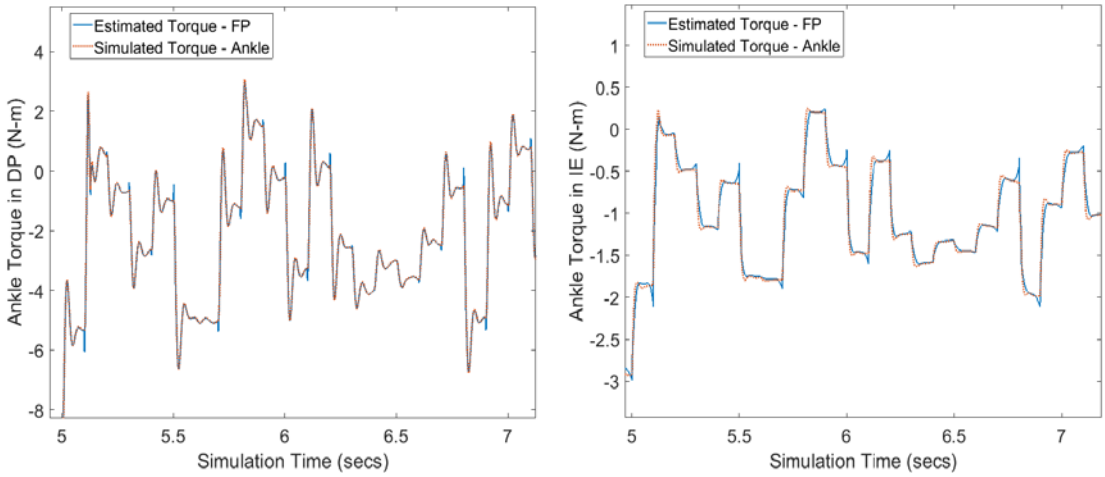

Figure 11. Error in estimation of ankle torque with ankle stiffness of 319 N-m/rad and 119 N-m/rad in DP and IE respectively

5.2. Position Control using Proportional-Integral-Derivative (PID)

Experimentally obtained trajectory of the ankle in the stance and swing phases was used as the reference trajectory for the simulation. The force plate was actuated using stochastic torque input data, which was used in the experiments. The stiffness and damping parameters of the revolute joints representing the hip and knee and the prismatic joints representing translation in X, Y and Z axes were set to zero. The ankle joint was active and its stiffness and damping in DP and IE directions was modulated as per the stage of the stance phase. Experimentally estimated impedance of the ankle at five instances of the stance phase [26] was used as the time-varying stiffness and damping values for the ankle joints in DP and IE. The simulation generates the ankle translational trajectory which was similar to the experimental data during the stance and swing phase, as shown in *Figure 12*. *Figure 13* shows the absolute error in the translational trajectory of the ankle with a mean relative error of 3.87±1% in the vertical translational position. The maximum relative error of 6.51% in the vertical translational position of the ankle occurs in the later part of the stance phase. This is possibly due to the inability of the foot model to perform toe-flexion (movement about metatarsophalangeal joints), which causes a difference in the gait trajectory. The ground reaction forces exerted by the ground surface and the force plate on the foot modulated the ankle translational and angular trajectories. *Figure 14* shows the experimental and simulated angular trajectories of the ankle. The absolute errors in tracking the ankle angular trajectories in DP and IE are shown in *Figure 15*. The mean relative error was 5.74±4.85% in DP and 4.94±3.13% in IE. The ground reaction forces experienced by the foot results in a reactive torque exerted by the force plate on the ankle. The resulting torque acting on the ankle in DP and IE during the stance phase was also fairly similar to the experimental data during the stance phase. *Figure 16* shows torque acting on the ankle in DP and IE. The simulated torque does not track the experimentally obtained torque with a high accuracy. This may be due to the inability of the ground contact model to vary its stiffness and damping according to the forces exerted on the ground surface due to the weight of the prosthesis.

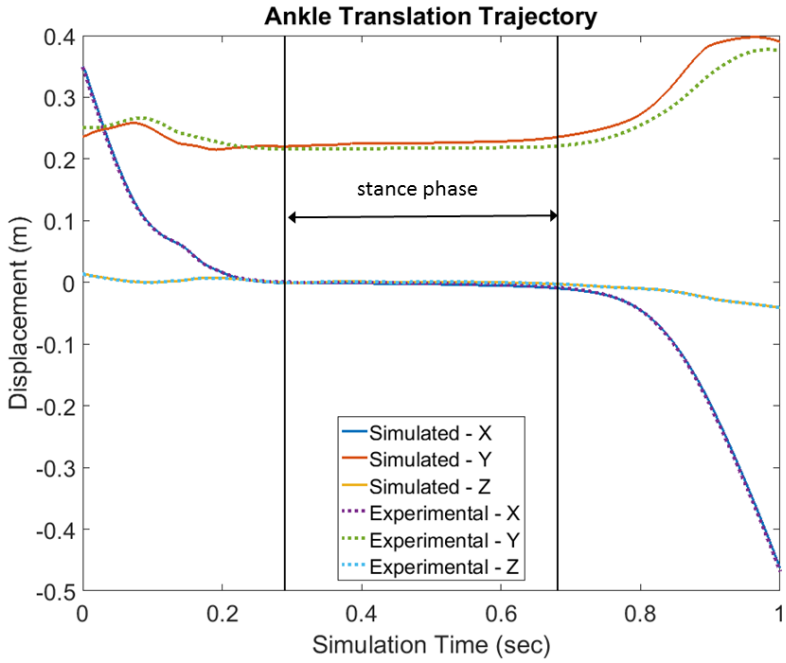

Figure 12. Translational trajectory of the ankle

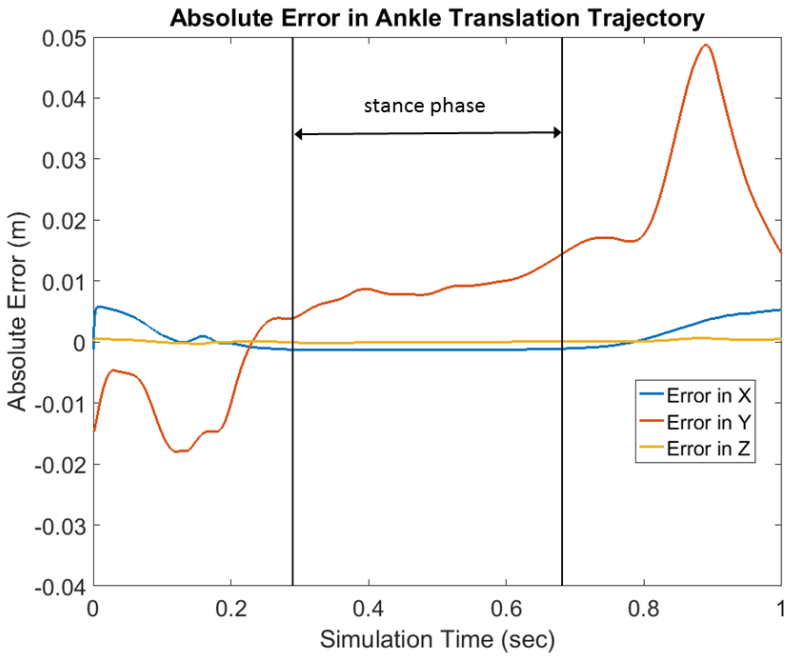

Figure 13. Absolute Error in translational trajectory of the ankle

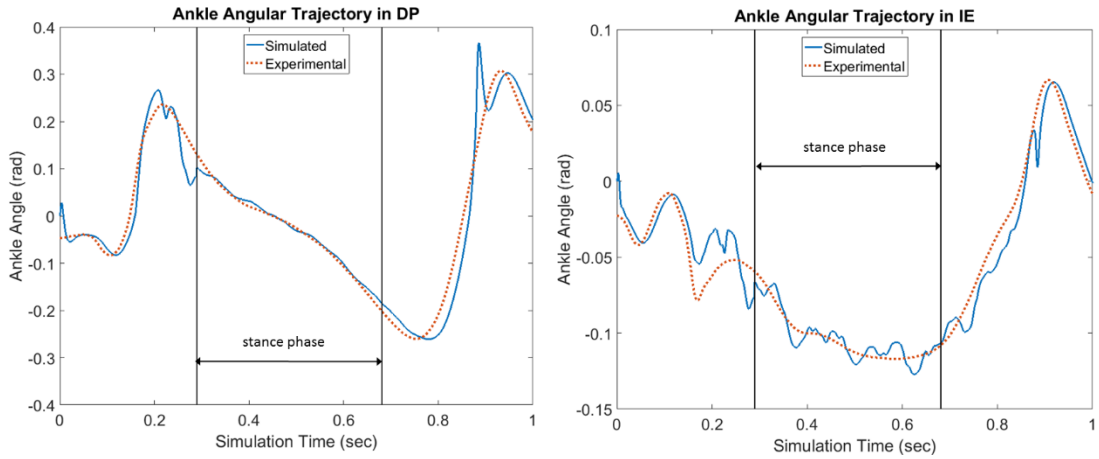

Figure 14. Angular trajectory of the ankle in DP and IE

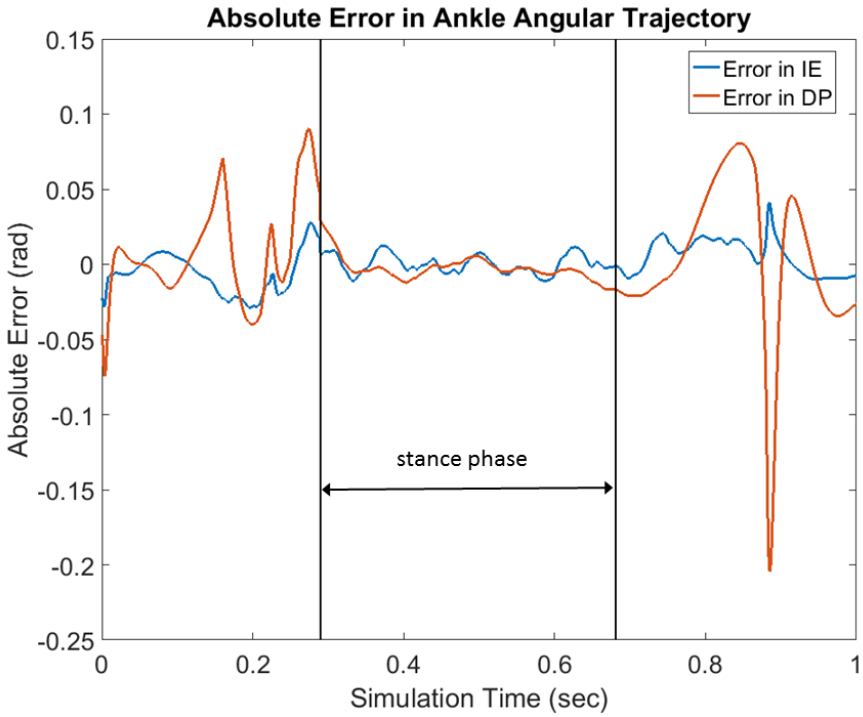

Figure 15. Error in angular trajectory of the ankle in DP and IE

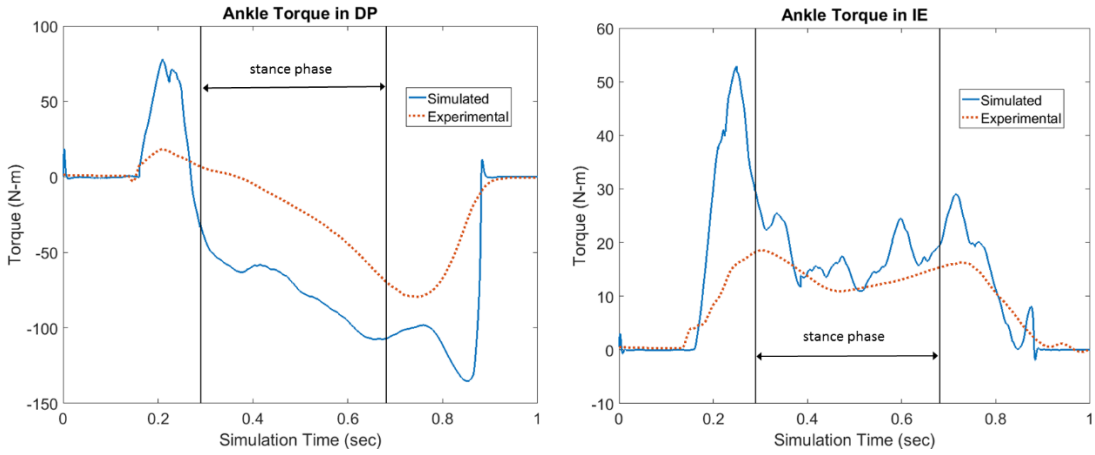

Figure 16. Torque acting on the ankle in DP and IE

5.3. Impedance Control

The stiffness and damping parameters of the revolute joints representing the hip and knee and the prismatic joints representing translation in X, Y and Z axes were set to zero. The impedance ankle joint was updated according to the stage of the stance phase. The ankle joint was active and actuated using torque computed by the impedance controller. The force plate was excited using stochastic torque used in the experiments. Implementing inverse kinematics and using experimentally obtained trajectory of the shank, the translational trajectory of the ankle was computed. The position, velocity and acceleration data of the foot was used as the reference trajectory for the end-effector. The impedance curve used in PID control method was used as the impedance of the ankle joint during the stance phase. The simulation produces ankle translational trajectory similar to the experimentally obtained reference trajectory as shown in *Figure 17*. The error in translational trajectory of the ankle during stance phase is shown in *Figure 18*. The mean relative error in the vertical translational trajectory during the stance phase was 0.53±0.3%. The simulation fairly tracks the angular trajectories of the ankle in DP and IE in the later phase of stance as shown in *Figure 19* with the absolute errors shown in *Figure 20*. The mean relative error in tracking angular trajectories was 37.58±31.9% in DP and 11.57±8.26% in IE. The relatively high error is due to tracking of the impedance of the ankle and not its trajectory during the stance phase. In order to maintain a certain impedance, the torque acting on the ankle is modulated which results in a different angular trajectory of the ankle. *Figure 21* shows the torque acting on the ankle in DP and IE. Although, the error in torque is higher during toe-off, the simulation generates a torque fairly similar to the experimentally obtained results for the remainder of the stance phase. This error is due to the inability of the foot model to simulate the flexion of the toes which generates the torque required for driving the prosthesis forward.

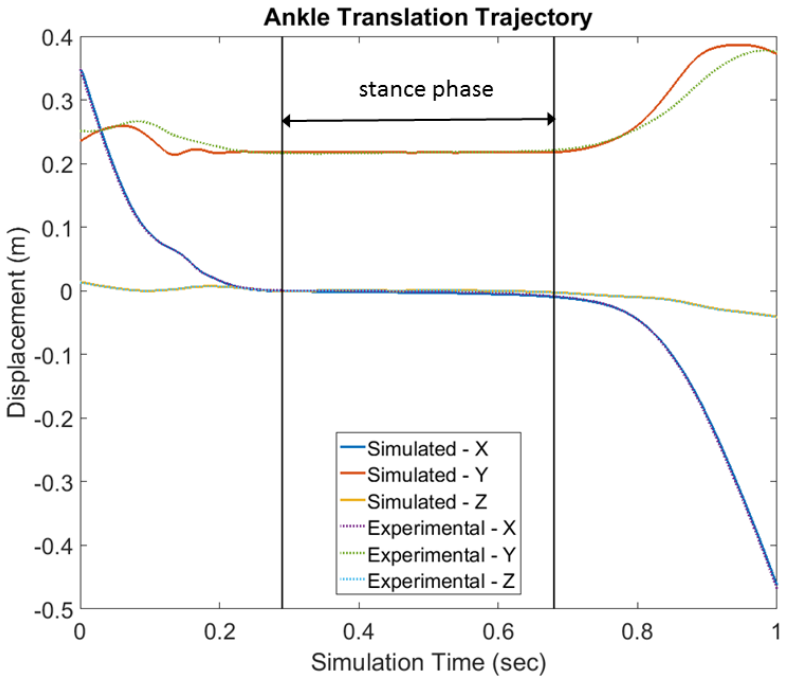

Figure 17. Translational trajectory of the ankle

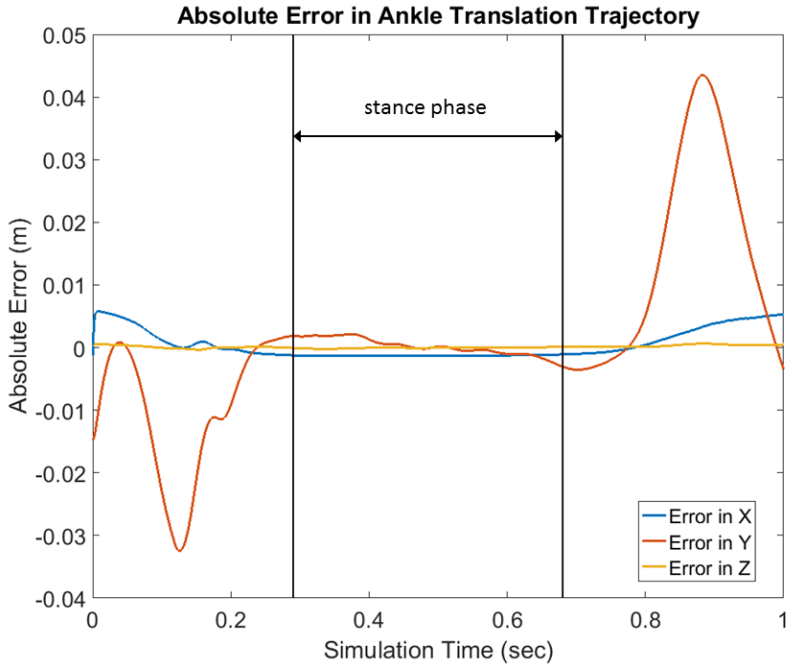

Figure 18. Absolute Error in translational trajectory of the ankle

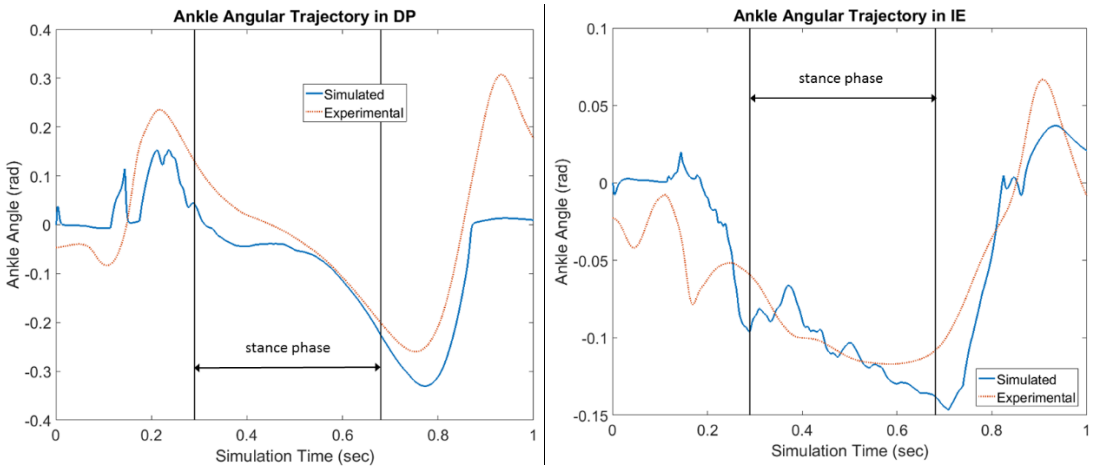

Figure 19. Angular trajectory of the ankle in DP and IE

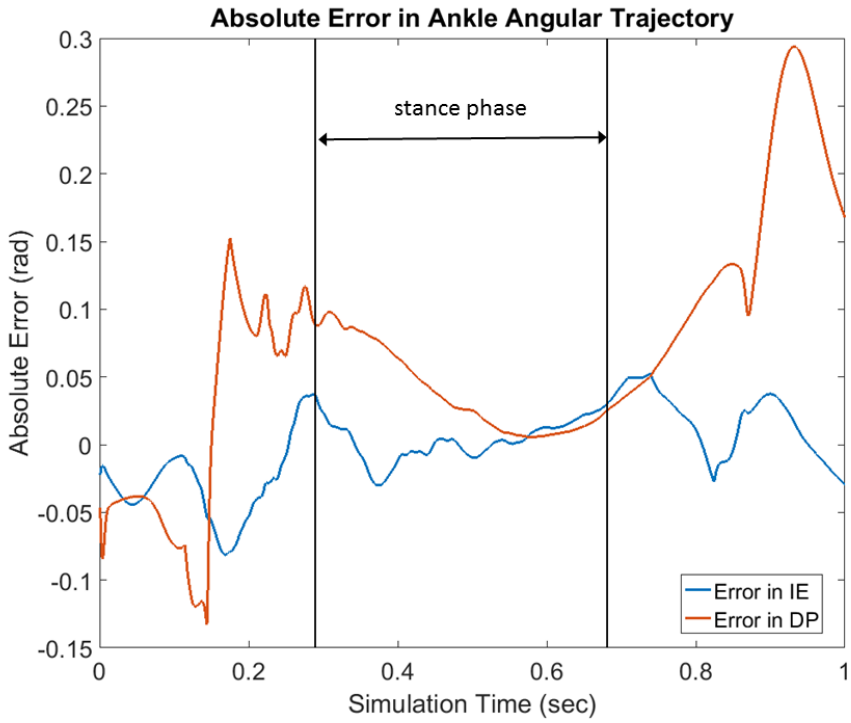

Figure 20. Error in angular trajectory of the ankle in DP and IE

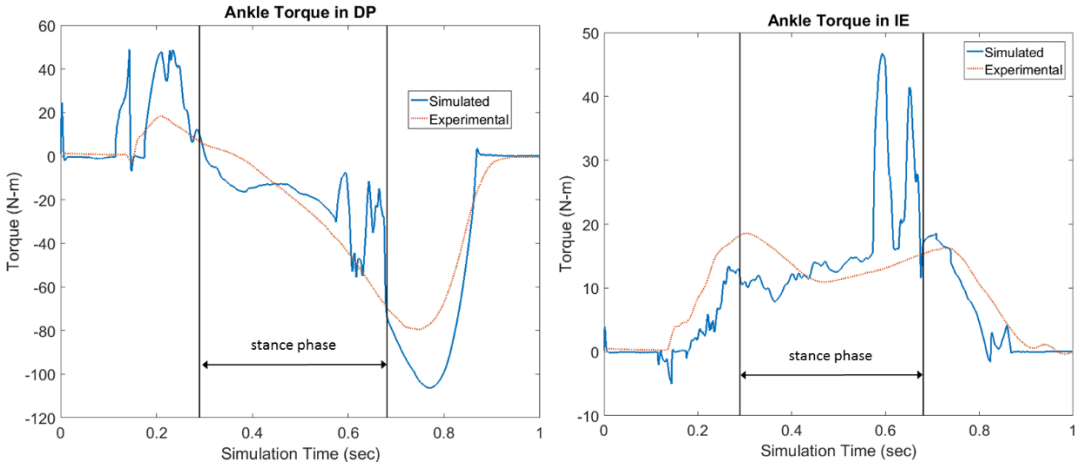

Figure 21. Torque acting on the ankle in DP and IE

6. Conclusion

The simulation developed mimics the ankle trajectory of an individual based on experimentally obtained straight walking trajectories of the human ankle. The simulation models a two-degree of freedom prosthesis and an instrumented walkway that was used in the experiments conducted on human participants to estimate their ankle impedance. The simulation was built using ankle trajectory data from two individuals and tested using data obtained from two additional individuals. Inverse kinematics was used to compute the trajectory of the knee and the hip joints along with the translation of the prosthesis. A ground contact model was developed to imitate the corporeal interaction of the foot of the prosthesis with the ground surface. Three controls methods were implemented to reproduce the individual's gait pattern, namely; positon control, proportional-integral-derivative (PID) control, and impedance control. Although providing undesirable results, position control aided the understanding of the foot-ground contact dynamics. Using time-varying impedance data of the ankle during stance phase and implementing PID control on the ankle joint, the simulation generates the human ankle trajectory with a mean error of 3.87±1% in the vertical translational position, and a mean relative angular position error of 5.74±4.85% in DP and 4.94±3.13% in IE. It also tracks the torque acting on the ankle, which validates the ground contact model. An impedance controller was employed to track the time-varying impedance of the ankle. The impedance controller mimicked the ankle trajectories with a mean relative error of 0.53±0.3% in the vertical translational position of the ankle joint. The impedance control method produced torque on the ankle similar to the experimental results with a maximum error occurring at toe-off. The simulation thus reproduces an individual's ankle trajectory satisfactorily and implicates the need for toe-flexion.

7. Future Work

This simulation was developed for straight walking gait trajectories. Since, the simulation allows for alteration of the orientation of the force plate, it can simulate different gait scenarios such as walking on tilted surfaces, side-step and turning steps. In future, it could simulate other gait maneuvers that include but are not limited to walking on uneven terrain, and ascending or descending stairs. In addition, as the weight of the prosthesis can be altered, the effect of the weight of an individual on their gait pattern can also be determined. This could help in simulating experiments where participants have to walk with different loads on their shank, foot and hip. The ground contact model could be enhanced by implementing toe-flexion motion in the foot model which would better imitate the real-time interaction of the foot with the ground surface. The simulation could help develop an impedance controller that varies the impedance of the ankle by using a generalized gait trajectory of the ankle, obtained by averaging ankle trajectories of a large number of individuals, allowing the foot to conform to the changes in profile of the ground surface. The simulation exhibits flexibility in employing other control methods, which can be initially tested on the simulation before implementing them on the prosthesis. By varying the impedance of the ankle in real-time, the simulation could help identify areas of the human ankle trajectory that play a major role in modulation of the ankle impedance.

References

[1] Ficanha EM, Rastgaar M, Kaufman KR, “Ankle mechanics during sidestep cutting implicates need for 2-degrees of freedom powered ankle-foot prostheses,” J Rehabil Res Dev. 2015; 52(1):97–112.
http://dx.doi.org/10.1682/JRRD.2014.02.0043

[2] Ficanha EM, Ribeiro G, Rastgaar Aagaah M, “Instrumented Walkway for Estimation of the Ankle Impedance in Dorsiflexion-Plantarflexion and Inversion-Eversion During Standing and Walking,” ASME. Dynamic Systems and Control Conference, Volume 3: V003T42A001.
https://doi.org/10.1115/DSCC2015-9774.

[3] Ziegler-Graham K, MacKenzie EJ, Ephraim PL, Travison TG, Brookmeyer R, “Estimating the Prevalence of Limb Loss in the United States: 2005 to 2050,” Archives of Physical Medicine and Rehabilitation2008; 89(3):422-9.
https://doi.org/10.1016/j.apmr.2007.11.005

[4] Colborne GR, Naumann S, Longmuir PE, Berbrayer D, “Analysis of mechanical and metabolic factors in the gait of congenital below knee amputees. A comparison of the SACH and Seattle feet,” Am J Phys Med Rehabil 1992; 71(5):272-78.
http://dx.doi.org/10.1097/00002060-199210000-00004

[5] Molen NH, “Energy-speed relation below-knee amputees walking on motor-driven tread1nill,” Int Z Angew Physiol, 1973; 31(3):173-85.

[6] Herr HM, Grabowski AM, editors, “Powered ankle-foot prosthesis improves metabolic demand of unilateral transtibial amputees during walking,” Proceedings of the 2011 Annual Meeting of the American Society of Biomechanics; 2012 Feb 7; 279(1728): 457–464.

[7] Ferris AE, Aldridge JE, Sturdy JT, Wilken JM, editors, “Evaluation of the biomimetic properties of a new powered ankle-foot prosthetic system,” Proceedings of the 2011 Annual Meeting of the American Society of Biomechanics; 2011; Long Beach (CA).

[8] Glaister BC, Orendurff MS, Schoen JA, Bernatz GC, Klute GK, “Ground reaction forces and impulses during a transient turning maneuver,” J Biomech. 2008; 41(14):3090- 93.
https://doi.org/10.1016/j.jbiomech.2008.07.022

[9] Hansen AH, Childress DS, Miff SC, Gard SA, Mesplay KP, “The human ankle during walking: Implications for design of biomimetic ankle prostheses,” J Biomech. 2004; 37(10):1467- 74.
https://doi.org/10.1016/j.jbiomech.2004.01.017

[10] Palmer ML, “Sagittal plane characterization of normal human ankle function across a range of walking gait speeds,” [Thesis], Cambridge, MA: Massachusetts Institute of Technology; 2002.

[11] Gates DH, “Characterizing ankle function during stair ascent, descent, and level walking for ankle prosthesis and orthosis design,” [Thesis]. Boston, MA: Boston University; 2004.

[12] Davis R, De Luca P, “Gait characterization via dynamic joint stiffness,” Gait Posture. 1996; 4(3):224- 31.
https://doi.org/10.1016/0966-6362(95)01045-9

[13] Arndt A, Wolf P, Liu A, Nester C, Stacoff A, Jones R, Lundgren P, Lundberg A, “Intrinsic foot kinematics measured in vivo during the stance phase of slow running,” J Biomech. 2007; 40(12):2672-78.
https://doi.org/10.1016/j.jbiomech.2006.12.009

[14] Ventura JD, Segal AD, Klute GK, Neptune RR, “Compensatory mechanisms of transtibial amputees during circular turning,” Gait Posture. 2011; 34(3):307- 12.
https://doi.org/10.1016/j.gaitpost.2011.05.014

[15] Ficanha E. M., Rastgaar M., “Preliminary design and evaluation of a multi-axis ankle–foot prosthesis,” 5th IEEE RAS/EMBS International Conference on Biomedical Robotics and Biomechatronics, BioRob (2014), pp:1033-1038
https://doi.org/10.1109/BIOROB.2014.6913916

[16] Shamaei K, Sawicki GS, Dollar AM, “Estimation of quasi-stiffness and propulsive work of the human ankle in the stance phase of walking,” PLoS ONE. 2013; Vol. 8(3):e59935.

[17] Rastgaar MA, Ho P, Lee H, Krebs HI, Hogan N, “Stochastic estimation of multi-variable human ankle mechanical impedance,” Proceedings of the ASME Dynamic Systems and Control Conference; 2009, DSCC2009, 2010, pp.957-959

[18] Rastgaar MA, Ho P, Lee H, Krebs HI, Hogan N, “Stochastic estimation of the multi-variable mechanical impedance of the human ankle with active muscles,” Proceedings of the ASME Dynamic Systems and Control Conference; DSCC2010, 2010, Vol.1, pp.429-431

[19] Lee H, Ho P, Krebs HI, Hogan N, “The multi-variable torque-displacement relation at the ankle,” Proceedings of the ASME Dynamic Systems and Control Conference; 2009, DSCC2009, 2010, pp.49-51.

[20] Lee H, Ho P, Rastgaar MA, Krebs HI, Hogan N, “Quantitative characterization of steady-state ankle impedance with muscle activation,” Proceedings of the ASME Dynamic Systems and Control Conference; DSCC2010, 2010, Vol.1, pp.321-323.

[21] Lee H, Ho P, Rastgaar MA, Krebs HI, Hogan N, “Multivariable static ankle mechanical impedance with relaxed muscles,” J Biomech. 2011; 44(10):1901-8. https://doi.org/10.1016/j.jbiomech.2011.04.028

[22] Lee H, Ho P, Rastgaar M, Krebs H, Hogan N, “Multivariable static ankle 1nechanical impedance with active muscles,” IEEE Trans. Neural. Syst. Rehabil. Eng. 2013;22(1):44-52.

[23] Rouse EJ, Hargrove LJ, Perreault EJ, Kuiken TA, “Estimation of human ankle impedance during walking using the perturberator robot,” Proceedings of the 4th IEEE RAS & EMBS lnternational Conference on Biomedical Robotics and Biomechatronics (BioRob); June 2012, pp.373-378.

[24] Rouse EJ, Hargrove LJ, Perreault EJ, Peshkin MA, Kuiken TA, "Development of a mechatronic platform and validation of methods for estimating ankle stiffness during the stance phase of walking," J Biomech Eng. 2013;135(8):81009. https://doi.org/10.1115/1.4024286

[25] Ficanha EM, Ribeiro GA, Dallali H and Rastgaar M (2016), "Design and Preliminary Evaluation of a Two DOFs Cable-Driven Ankle–Foot Prosthesis with Active Dorsiflexion–Plantarflexion and Inversion–Eversion," Front. Bioeng. Biotechnol. Vol. 4, pp.36. https://doi.org/10.3389/fbioe.2016.00036

[26] Ficanha M., Ribeiro G., Knop L., Rastgaar M., "Time-Varying Human Ankle Impedance in the Sagittal and Frontal Planes during Stance Phase of Walking," IEEE International Conference on Robotics and Automation (ICRA), May 29 – June 3, 2017, Singapore.

[27] Hogan N, "Impedance Control: An Approach to Manipulation," IEEE American Control Conference, 1984, Vol.1, pp.304-313

[28] Robotran, Center for Research in Mechatronics (CEREM) of the Université catholique de Louvain (UCL), Louvain-la-Neuve, Belgium.

[29] LabVIEW®, National Instruments Corporation, Austin, TX

[30] MATLAB® Release 2015a, The MathWorks, Inc., Natick, Massachusetts, United States.

[31] Dassault Systèmes SOLIDWORKS Corp., Waltham, Massachusetts, USA

[32] Aguiar L, Santos-Rocha R, Veloso Antonio, "Prediction of Ground Reaction Forces during Gait using Simulation Analysis," Journal of Biomechanics; July 2012, Vol.45, supplement 1, pp.S239.

[33] Glaister BC, Bernatz GC, Klute GK, Orendurff MS., "Video task analysis of turning during activities of daily living," Gait Posture; February 2007; Vol. 25(2), pp.289-294.